

Robust Model Predictive Control Applied to an ESP-lifted Oil Well System

Bruno A. Santana* Victor S. Matos* Daniel D. Santana**
Márcio A. F. Martins*,**

* *Mechatronics Program, Polytechnic School, Federal University of Bahia, BA, (e-mail: {bruno.aguiar,victosm}@ufba.br).*

** *Department of Chemical Engineering, Polytechnic School, Federal University of Bahia, BA (e-mail: {daniel.diniz,marciomartins}@ufba.br).*

Abstract: This work presents the first robust model predictive control approach for controlling an Electric Submersible Pump (ESP) lifted oil well system considering its benefits and operational envelope constraints. The proposed scheme is based on a robust infinite horizon model predictive controller (RIHMPC) with multi-model formulation as the uncertainty description and zone control scheme to explicitly consider the time-varying ESP (downthrust and upthrust) envelope constraints. The proposed control strategy is tested through simulation for the disturbances commonly found in the oil wells with ESP installations and (nonlinear) plant/model mismatch scenarios. Results show an applicable formulation capable of accommodating nonlinearities in the form of uncertainties and a low computational cost, with characteristics suitable for real-time applications.

Keywords: Artificial Lift Methods, Electric Submersible Pump (ESP), Robust Model Predictive Control, Robust Control.

1. INTRODUCTION

The second most widely used artificial lift method is the Electric Submersible Pump, which increases the flow rate of oil wells, being a method that can yield the highest oil production (Zhu and Zhang, 2018). Its operation must satisfy the operational envelope, a phase portrait formed by downthrust and upthrust constraints, through the adjustment of the pump rotational speed and the opening of the production choke valve (Fontes et al., 2020).

Some development in control techniques for ESP-lift systems can be observed in the literature, mainly focused on model predictive control (MPC), which systematically handle typical system constraints. Pavlov et al. (2014) proposed an MPC controller for an ESP-lifted oil well facility to track the ESP intake pressure and minimize the power consumption by applying a target to the choke valve opening. Their formulation also considered the envelope operation constraints. In a similar formulation, Binder et al. (2014) proposed an embedded MPC on a programmable logic controller with hardware-in-the-loop simulations to track the flow rate and indirectly minimize the ESP power consumption by regulation of the motor current. They did not consider the envelope constraints. Another MPC application was proposed in Krishnamoorthy et al. (2016), based on the same control objectives of Pavlov et al. (2014), but with a linearized model from a high fidelity ESP simulator with heavy viscous crude oil. The robustness of the control application was evaluated, and it was able to deal even with fluid viscosity changes.

Patel et al. (2018) presented the first practical implementation of MPC in a real oilfield with multiple ESP-lifted systems resulting in power savings from 10% to 20%. Their control law considered the flow rate set-point tracking and practical ESP constraints, using the rotational speed, the choke valve opening, and the ESP voltage as manipulated variables. Binder et al. (2019) include feed-forward action to previous works (Pavlov et al., 2014; Binder et al., 2014) considering measured disturbances, such as reservoir pressure of the ESP-lifted oil well system, in order to evaluate the improvement of the control performance.

The aforementioned works presented conventional formulations of MPC, focused on the region of operation for which they were proposed. Delou et al. (2019a) extended the control operation range and robustness of predictive controllers using an adaptive formulation based on a linear combination of two models, without explicitly considering the upthrust and downthrust constraints. After that, Delou et al. (2019b) proposed an adaptive multiple-model formulation, where the model of the state estimator is also updated, forming a robust approach for losing measurements of state variables. Delou et al. (2020) compared two switch strategies of interpolations for the state estimation with equivalent results.

Furthermore, Fontes et al. (2020) presented the first application of stabilizing MPC in an ESP-lifted oil well system, using a zone approach to deal with envelope constraints, with economic targets and guaranteed feasibility, but limited to a single linear model. Santana et al. (2021b) extended this work through successive linearizations of the model, forming an adaptive formulation applied to

the zone MPC with guaranteed feasibility. Santana et al. (2021a) presented another extension of Fontes et al. (2020), being the first work to embed this zone MPC formulation on a low-cost and low memory microcontroller focusing on an ESP-lifted oil system.

Regarding robust MPC formulations applied to ESP system, only Delou et al. (2019b) and Delou et al. (2020) proposed a called robust MPC approach associated with lack of state variables measurements, not related with model uncertainties. Therefore, this work presents the extension of the zone MPC (González et al., 2009) to the robust case by explicitly considering a description of uncertainties formed by different models for a set of operating conditions, taking into account the envelope constraints in a zone control approach in a structure that can be implemented in practice. Slack variables related to the problem constraints guarantee the robust stabilizing properties and feasibility of the optimization problem, which is a fundamental property when envisioning future embedded applications. This work can be considered the first explicitly robust approach of MPC applied to an ESP system, capable of dealing with a set of operating conditions.

This work is organized as follows. Section 2 briefly describes the ESP-lifted oil well system and its dynamic model. Section 3 presents the proposed robust control scheme. Section 4 presents a case study of applying the proposed control strategy for different disturbance scenarios and plant/model mismatch of the ESP system. Finally, Section 5 concludes the paper.

2. THE ESP MODEL

A typical ESP-lifted oil well system is presented in Figure 1, whose variables are described from the associated mass and moment balance equations, summarized in (1). The ESP operation is based on manipulating the pump rotational frequency (f) and the opening of the production choke valve (z_c) to control the additional pressure applied to the oil and forcing it to rise to the surface. The so-called operational envelope comprises time-variant upthrust and downthrust constraints, which rely on fluid properties, flow type, the average flow rate in the production column (q_p) and ESP head (H) dynamics. In this work, we consider the average flow of the production column as a measured variable, thus, at each sampling interval, the maximum (H_{max}) and minimum (H_{min}) head values are defined for the current value of q_p in the operational envelope curve.

The dynamic model of the ESP-lifted oil well proposed in Pavlov et al. (2014) is used for the dynamic simulation of the ESP-lifted oil well system and is described as differential-algebraic equations as follows:

$$\begin{cases} \dot{p}_{wh} = 1.54 \times 10^8 (q_p - q_c) \\ \dot{p}_{bh} = 0.8584 (p_r - p_{bh}) - 3.7 \times 10^8 q_p \\ \dot{q}_p = 5.02 \times 10^{-9} [p_{bh} - p_{wh} - 6.30 \times 10^8 q_p^{1.75} \\ \quad + 9.32 \times 10^3 (H - 1 \times 10^3)] \\ q_c = 2 \times 10^{-3} z_c \sqrt{p_{wh} - p_m} \\ p_{in} = p_{bh} - 1.85 \times 10^8 q_p^{1.75} - 1.9 \times 10^6 \\ H = 0.2664 f^2 + 133.09 f \cdot q_p - 1.41 \times 10^6 q_p^2 \end{cases} \quad (1)$$

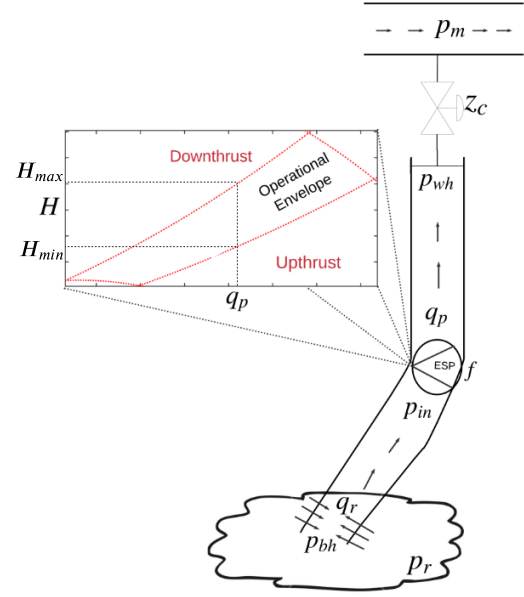


Figure 1. Scheme of an ESP-lifted oil production system (Fontes et al., 2020).

where p_{bh} , p_{wh} , p_{in} , p_m are the bottom hole, wellhead, intake and manifold pressures, respectively; q_c are the production choke flow rates, respectively.

3. PROPOSED ROBUST MPC SCHEME FOR ESP

The robust control scheme proposed here is based on a multi-model approach, in which a set of L possible linear models of the ESP dynamic are specified for some operational points. The Robust Infinite Horizon Model Predictive Control (RIHMPC), firstly presented in Odloak (2004) and extended to the zone approach in González et al. (2009), enforces a non-increasing cost constraints for each of the models of the set, but the cost function is minimized solely for a selected nominal model (González et al., 2009). The RIHMPC formulation achieves robust stability with the feasibility of the optimization problem by using slack variables (Odloak, 2004).

The RIHMPC with zone control aims to solve the following optimization problem at each time step k :

Problem P1

$$\begin{aligned} & \min_{\Delta \mathbf{u}_k, \mathbf{y}_{sp,k}(\Theta_n=1, \dots, L), \delta_{y,k}(\Theta_n=1, \dots, L), \delta_{u,k}} V_k(\Theta_N) \\ V_k(\Theta_N) = & \sum_{j=0}^m \|\mathbf{y}_N(k+j|k) - \mathbf{y}_{sp,k}(\Theta_N) - \delta_{y,k}(\Theta_N)\|_{\mathbf{Q}_y}^2 + \\ & + \|\mathbf{x}_N^{st}(k+m|k)\|_{\mathbf{Q}(\Theta_N)}^2 + \sum_{j=0}^{m-1} \|\mathbf{u}(k+j|k) - \mathbf{u}_{tg,k} - \delta_{u,k}\|_{\mathbf{Q}_u}^2 + \\ & + \sum_{j=0}^{m-1} \|\Delta \mathbf{u}(k+j|k)\|_{\mathbf{R}}^2 + \|\delta_{y,k}(\Theta_N)\|_{\mathbf{S}_y}^2 + \|\delta_{u,k}\|_{\mathbf{S}_u}^2, \end{aligned}$$

subject to:

$$\begin{aligned} & -\Delta \mathbf{u}_{max} \leq \Delta \mathbf{u}(k+j|k) \leq \Delta \mathbf{u}_{max}, \quad j = 0, \dots, m-1, \quad (2) \\ & \mathbf{u}_{min} \leq \mathbf{u}(k+j|k) \leq \mathbf{u}_{max}, \quad j = 0, \dots, m-1, \quad (3) \\ & \mathbf{u}(k+m-1|k) - \mathbf{u}_{tg,k} - \delta_{u,k} = \mathbf{0}, \quad (4) \end{aligned}$$

and, for each $n = 1, \dots, L$,

$$\mathbf{y}_{\min,k} \leq \mathbf{y}_{sp,k}(\Theta_n) \leq \mathbf{y}_{\max,k}, \quad (5)$$

$$\mathbf{x}_n^s(k+m|k) - \mathbf{y}_{sp,k}(\Theta_n) - \delta_{y,k}(\Theta_n) = \mathbf{0}, \quad (6)$$

$$V_k(\Theta_n) \leq \tilde{V}_k(\Theta_n), \quad (7)$$

where Θ_N represents the most likely model (or nominal) of the set of L models, m is the control horizon, $\mathbf{y}(k+j|k)$ are the predictions of the controlled variables at time step $k+j$ given the information at time step k . $\Delta \mathbf{u}(k+j|k)$ are increments on manipulated variables, $(\mathbf{u}_{\min}, \mathbf{u}_{\max})$, $\Delta \mathbf{u}_{\max}$ are the bounds of manipulated variables and increments on manipulated variables, respectively. $(\mathbf{y}_{\min}, \mathbf{y}_{\max})$ are the zone specification for the controlled variables and $\mathbf{y}_{sp,k}$ are the output set-points within the zone control scheme imposed by (5). $\mathbf{x}_n^s(k+m|k)$ are the integrating states produced by the incremental form of inputs in the state space for the L models. \mathbf{Q}_y and \mathbf{R} are the weighting matrices of (ny) controlled variables and the increment of (nu) manipulated variables, respectively. $\Delta \mathbf{u}_k = [\Delta \mathbf{u}^T(k|k) \dots \Delta \mathbf{u}^T(k+m-1|k)]^T$ is the control actions vector; $\delta_{y,k} \in \mathbb{R}^{ny}$ and $\delta_{u,k} \in \mathbb{R}^{nu}$ are the slack variables used to guarantee the feasibility of the optimization *Problem 1*. $\mathbf{S}_y \in \mathbb{R}^{ny \times ny}$ and $\mathbf{S}_u \in \mathbb{R}^{nu \times nu}$ are the weighting matrices of the slack variables. \mathbf{u}_{tg} are input targets and \mathbf{Q}_u is their weighting matrix. $V_k(\Theta_n)$ is the actual cost function value for each model and $\tilde{V}_k(\Theta_n)$ is the cost function obtained with a solution inherited from *Problem 1* at time step $k-1$ and translated to time k . More details in Odloak (2004); González et al. (2009); Martins and Odloak (2016).

The robust stability guarantee is associated with constraint (7), which imposes the cost contraction for all models. The prediction model is based on a canonical state-space model formulation based on the analytical form of the step response of the system (Odloak, 2004), which has artificial integrating states to achieve offset-free tracking. In this way, the terminal constraints (6) and (4) (softened by slacks) must be part of the formulation to prevent the cost from becoming unbounded.

Note that *Problem 1* is a nonlinear optimization problem. However, it is a convex problem and, therefore, less computationally expensive than non-convex problems found in nonlinear MPC formulations. Figure 2 shows the implementation scheme of the RIHMPC in the ESP, where the controlled variables are the intake pressure and pump head (as zone approach with (H_{min}, H_{max}) limits defined by operational envelope time-varying constraint function of flow rate, as seen in Figure 1), considering the rotational speed and choke valve opening as manipulated variables.

Since the prediction models have unmeasured states, it is necessary to use L state estimators to infer the states for each model from the measurements of the plant. In this work, it was implemented linear Kalman filters as estimators, as seen in Figure 2. Furthermore, since the RIHMPC is based on the linear state-space models and the ESP is represented by nonlinear model (1), it is necessary to correct the mismatch effect, task also performed by the Kalman filter.

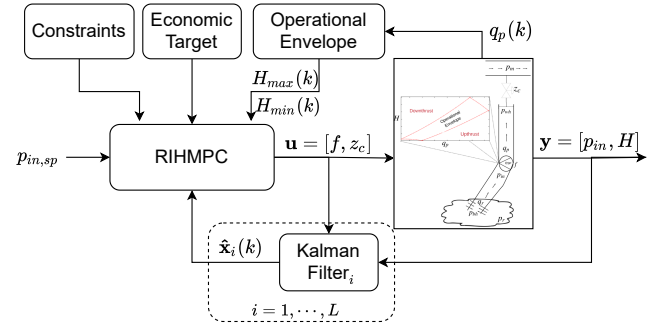


Figure 2. Scheme for application of the zone RIHMPC controller in the ESP-lifted oil well.

4. SIMULATION RESULTS

This section presents the proposed zone RIHMPC strategy in two scenarios of plant-model mismatch, with different operating conditions in the nonlinear ESP-lifted oil well system described as in (1). The control objectives adopted to ESP under proposed RIHMPC:

- (1) Tracking of set-point of the ESP intake pressure;
- (2) Holding safe operation inside the ESP operational envelope;
- (3) Evaluating robustness to tackle disturbances and deal with nonlinearities;
- (4) Minimization of the power consumption of the ESP motor.

In the control law of *Problem 1*, the RIHMPC is applied to track and maintain the intake pressure reference and to keep the pump head inside the operational envelope by the manipulation of the rotational frequency and choke valve opening. The first test scenario is focused on evaluation of objectives (1), (2) and (3). Then, the second test analyzes the objective (4) introducing the use of economic target in the choke valve opening.

The multi-model set Θ is defined by linearization of the ESP nonlinear model (1) for three different operating points: $f_{ss,1} = 35.29$ Hz, $z_{c_{ss,1}} = 14.53$ %; $f_{ss,2} = 55.44$ Hz, $z_{c_{ss,2}} = 31.58$ %; $f_{ss,3} = 65$ Hz, $z_{c_{ss,3}} = 98.97$ %. They are discretized with a sampling time of 2 seconds, forming $L = 3$ linear models in the canonical form. This amount of models map a wide operating range to the system, representing probable operating conditions of an ESP-lifted oil well system, and we sought to choose the smallest number of models to avoid increasing the computational burden. The tuning parameters of the RIHMPC controller used in the following simulations are: $m = 4$, $\mathbf{Q}_y = \text{diag}([100, 1000])$, $\mathbf{Q}_u = \text{diag}([0, 0])$, $\mathbf{R} = \text{diag}([100, 0.0001])$, $\mathbf{S}_y = \text{diag}([1, 0.01]) \times 10^4$, $\mathbf{S}_u = \text{diag}([0, 0])$ and the ESP constraints: $\mathbf{u}_{min} = [35 \text{ Hz}, 0 \text{ \%}]$, $\mathbf{u}_{max} = [65 \text{ Hz}, 100 \text{ \%}]$, $\Delta \mathbf{u}_{max} = [0.5 \text{ Hz/s}, 0.5 \text{ \% / s}]$. The zone specification $\mathbf{y}_{min}(k) = [p_{in,sp}(k), H_{min}(k)]$ and $\mathbf{y}_{max}(k) = [p_{in,sp}(k), H_{max}(k)]$, specifying set-point tracking for the intake pressure and min/max head from the operational envelope. The typical tuning parameters of the Kalman filters were defined as $\mathbf{Q}_{kf} = 0.5 \cdot \mathbf{I}_{14}$ and $\mathbf{R}_{kf} = \text{diag}([0.5, 0.5])$.

In the first simulation scenario, we investigated the controller performance under the conditions of reference tracking for intake pressure and unmeasured disturbance com-

compensation when the plant is affected by a disturbance related to a manifold pressure variation. To this end, we introduced a decrease of 50% in manifold pressure at 200 s, then an increase of 150% at 700 s, and finally an increase of 40% at 1200 s. Also, we consider that the plant is corrupted by measurement noises in the controlled variables with Gaussian distribution $\mathcal{N}(0, \mathbf{W})$, and $\mathbf{W} = \text{diag}([1.90 \text{ bar}^2, 23.81 \text{ m}^2])$.

Figure 3 displays the dynamic behavior of the intake pressure and shows that the controller is able to drive this variable to the desired references, even under different operating conditions. It is worth mentioning that the nominal model of the controller (model 1) was linearized in the region corresponding to the last set-point. Therefore, it is clear that the RIHMPC controller preserves a good performance for a wide operating range of the ESP system, unlike the conventional IHMPC strategy with a single nominal model, whose performance deteriorates when moving away from the linearization region, as evidenced in Santana et al. (2021b).

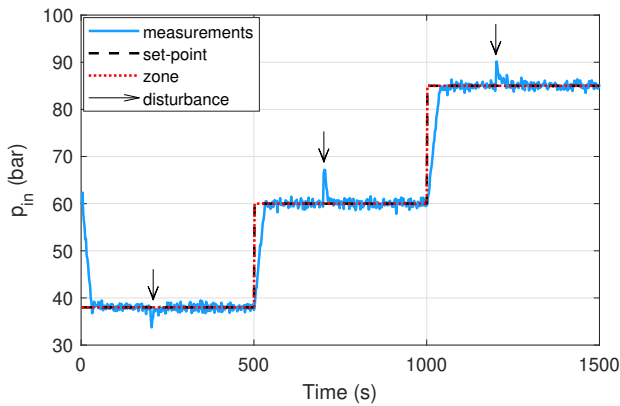


Figure 3. Dynamic of the intake pressure for RIHMPC controller formulation.

With regard to the envelope constraints, Figure 4 shows that this robust controller keeps the head within the zone throughout the simulation. However, after the disturbance input at instant 200 s, note that the system inevitably operates outside the envelope during a short period, then gradually returns to the zone. Also, note that the controller evaluates the output set-point as the minimum value of the zone - the upthrust constraint. This undoubtedly softens the optimization problem and guarantees the feasibility of the proposed zone RIHMPC scheme, unlike what would happen, for example, if we were to directly restrict the output predictions as it happens in classical MPC formulations (it will not produce a solution). Figure 6 provides another perspective on the system's trajectory in terms of the operational envelope, confirming that the controller keeps the system outside the envelope for a short time after the disturbance inputs.

The signal of manipulated variables produced by the RIHMPC controller fulfills the input constraints and reacts to compensate for the changes on input set-points and disturbances exciting the system, as seen in Figure 5. As the choke valve opening influences the nonlinearity of the ESP-lifted system more strongly, note that the controller made the system remains in a median region of z_c , more strongly associated with model 2. However, it maintained

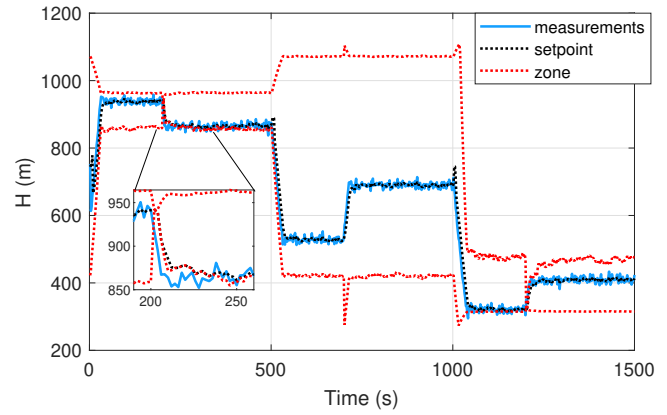


Figure 4. Dynamic of the Head and envelope time-varying constraint for RIHMPC controller formulation.

a robustly satisfactory performance considering model 1 as nominal

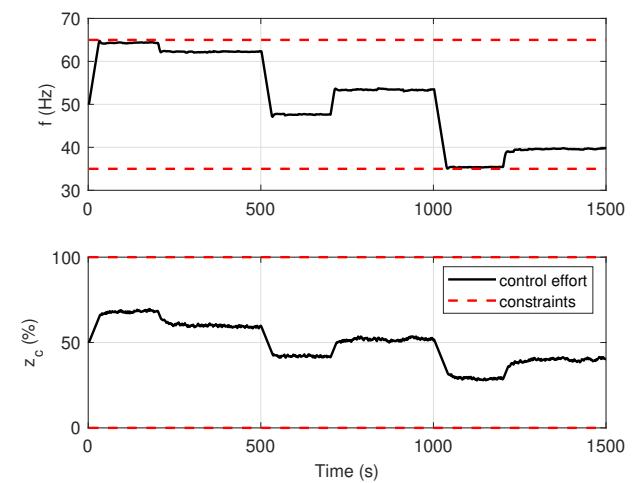


Figure 5. Signal of the manipulated variables.

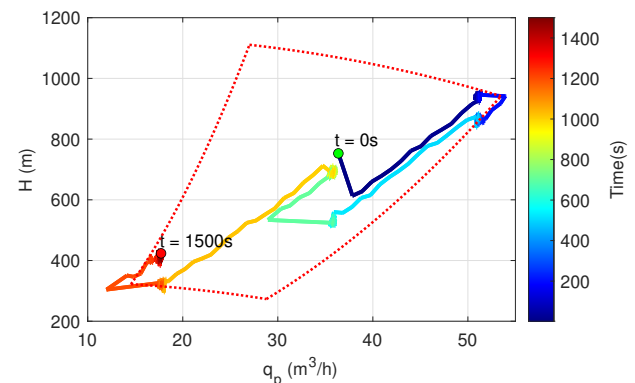


Figure 6. ESP operating envelop of the first simulation scenario.

As mentioned in section 3, slack variables play a crucial role in ensuring the feasibility of the optimization problem resulting from the RIHMPC control law. Figures 7 and 8 show that the output slack variables are necessary during the transient periods for all models of the uncertainty description set. However, they converge shortly after that. Furthermore, the cost function decreases, even when there is a plant-model mismatch. It is worth mentioning that the slack variables of each model represent the model's degree of error, shown by the difference between each model slack after disturbances and reference changes.

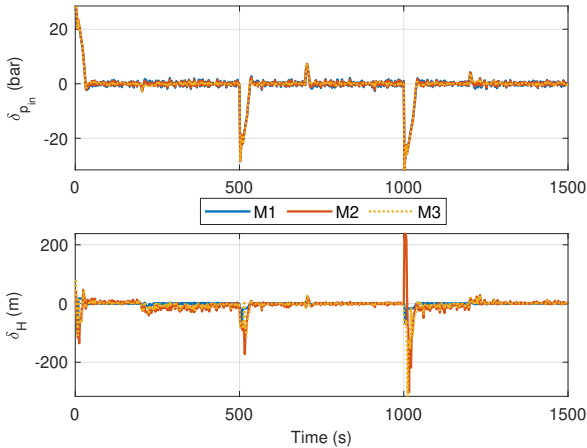


Figure 7. Output slack variables for the L models.

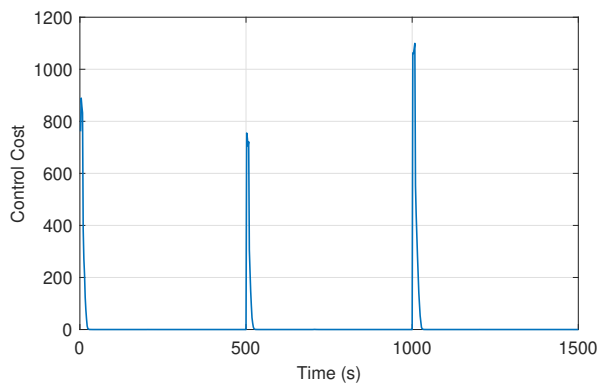


Figure 8. Cost function of the nominal model.

In this scenario, we evaluate the computational effort needed to calculate the nonlinear optimization problem, as described in *Problem 1*. The computational times of MATLAB's `fmincon` solver are presented in Figure 9, which is obtained on a computer with an AMD Ryzen 7 3700U, 12 Gb of RAM, and Windows 10 operating system. As can be seen, throughout the simulation, the computational times of *Problem 1* do not exceed the sampling interval considered in this case study, namely 2 s, thus proving to be perfectly viable for real-time implementation purposes. The worst-case execution time observed was 0.53 s, while the average computational time was only 0.22 s. We emphasize that this computational performance is related to the format of *Problem 1*, which despite being a nonlinear optimization, it is a convex problem, therefore, less computationally expensive.

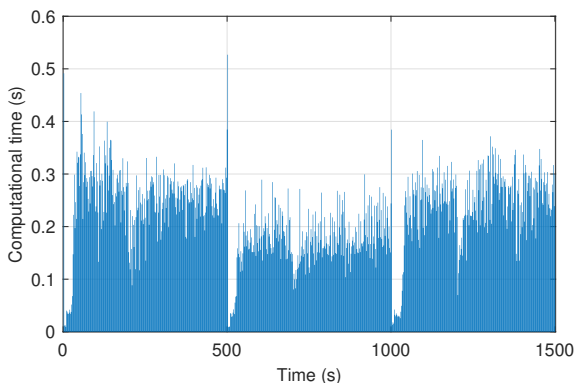


Figure 9. Computation time of the optimization problem.

In the next scenario it is evaluated the RIHMPC with active economic target $u_{tg} = z_c \rightarrow 90\%$. For this, the tuning parameters are modified to $\mathbf{Q}_u = [0, 1]$ and $\mathbf{S}_u = [0, 1]$. This situation corresponds to forcing the system to work in the region of maximum productivity operation, also associated with model 3, to minimize ESP energy consumption. The nominal model was maintained as the first model of Θ to simulate the worse situation for robustness evaluation.

The comparison between the performance of the controller with and without the use of the target in Figure 10 shows an equivalent dynamic for intake pressure, as expected, since this variable is prioritized in both cases. The $\text{target}_{\text{on}}$ controller worked with smaller rotational frequency of the ESP motor, and the choke valve opening converged to $z_{c,tg}$ as seen in Figure 11. The practical difference between ON/OFF target formulations lies in the fact that the ESP head reaches distinct steady-states, with different trajectories on the operational envelope, as seen in Figure 12. The computational effort of this scenario also respected the sampling interval, with a maximum time of 0.39 s for the $\text{target}_{\text{on}}$ formulation while the $\text{target}_{\text{off}}$ reaches 0.50 s.

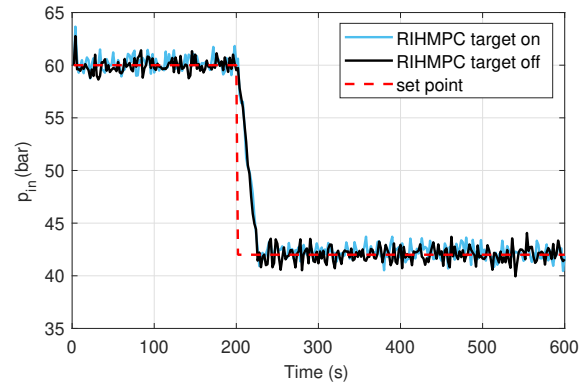


Figure 10. Intake pressure in the comparison of target application.

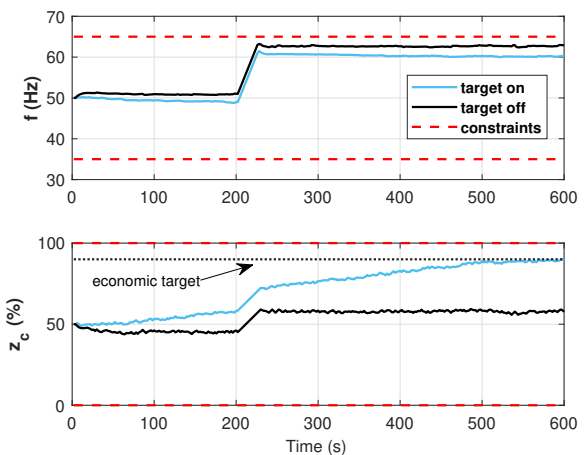


Figure 11. Manipulated variables of target comparison scenarios.

In order to ensure the feasibility to apply an input target, the constraint (4) is softened with the input slack so that the search for the target can be achieved when it is possible for the system operation, as seen in the Figure 13, showing the aforementioned convergence.

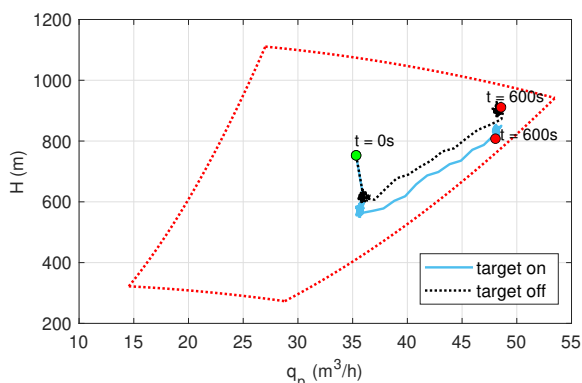


Figure 12. Envelope constraint of target comparison scenarios.

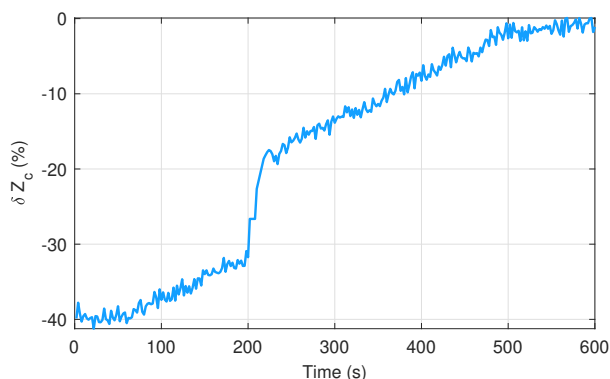


Figure 13. Valve opening input slack of target scenario.

If one considers the ESP power consumption through $P = C_p P_0 \left(\frac{f}{f_0}\right)^3$, where C_p is the viscosity correction factor, P_0 and f_0 are the reference power and frequency, it can be shown that the target_{on} RIHMPC yields a reduction of 9.47% in this index, while maintaining almost the same oil production: 7.3049 m³ with target OFF and 7.2677 m³ with target_{on}, achieving the desired economic benefits.

5. CONCLUSION

This work presented an explicitly robust MPC formulation that was not yet been explored in ESP oil production process installations. The control law allows including a set of system information, i.e., models, to form a robust formulation even in restricted scenarios, with a mismatch, nonlinearities, and disturbances. Also, accommodating the guarantee of feasibility by using slacked terminal constraints and successfully respecting the downthrust and upthrust ESP envelope operating constraints by incorporating artificial set-points of the zone control approach.

The results showed the benefits of the RIHMPC controller to all the nonlinearity of the ESP-lifted system, achieving satisfactory performance even outside the nominal region, as expected in a robust control formulation. In addition, the computational performance obtained shows that the formulation is viable for embedded applications, even in the case of a nonlinear optimization, which is the objective of future work.

ACKNOWLEDGEMENTS

The authors thank the ANP-FINEP within the scope of PRH 35.1-ANP and Coordenação de Aperfeiçoamento de Pessoal de Nível Superior - Brasil (CAPES) - Finance Code 001, for their financial support.

REFERENCES

- Binder, B.J., Johansen, T.A., and Imsland, L. (2019). Improved predictions from measured disturbances in linear model predictive control. *Journal of Process Control*, 75, 86–106.
- Binder, B.J., Kufalor, D.K., Pavlov, A., and Johansen, T.A. (2014). Embedded model predictive control for an electric submersible pump on a programmable logic controller. *2014 IEEE Conference on Control Applications, CCA 2014*.
- Delou, P.A., de Souza, M.B., and Secchi, A.R. (2020). Addressing the lack of measurements in the subsea environment by using a model scheduling Kalman filter coupled with a robust adaptive MPC. *Brazilian Journal of Chemical Engineering*, (0123456789).
- Delou, P., Azevedo, J., Krishnamoorthy, D., Souza, M., and Secchi, A. (2019a). Model predictive control with adaptive strategy applied to an electric submersible pump in a subsea environment. *IFAC-PapersOnLine*, 52(1), 784–789.
- Delou, P., Souza, M., and Secchi, A.R. (2019b). A Robust Adaptive MPC coupled with Kalman Filter for an Electric Submersible Pump System: A multi-model approach. *I Brazilian Congress on Process Systems Engineering (PSE-BR 2019)*, (2014), 435–438.
- Fontes, R., Costa, E., Abreu, O.L., Martins, M., and Schmitman, L. (2020). On application of a zone IHMPC to an ESP-lifted oil well system. In *Anais do Congresso Brasileiro de Automática 2020*.
- González, A., Marchetti, J., and Odloak, D. (2009). Robust model predictive control with zone control. *IET Control Theory & Applications*, 3(1), 121–135. doi:10.1049/iet-cta:20070211.
- Krishnamoorthy, D., Bergheim, E.M., Pavlov, A., Fredriksen, M., and Fjalestad, K. (2016). Modelling and Robustness Analysis of Model Predictive Control for Electrical Submersible Pump Lifted Heavy Oil Wells. *IFAC-PapersOnLine*, 49(7), 544–549.
- Martins, M.A. and Odloak, D. (2016). A robustly stabilizing model predictive control strategy of stable and unstable processes. *Automatica*, 67, 132–143.
- Odloak, D. (2004). Extended robust model predictive control. *AIChE Journal*, 50(8), 1824–1836.
- Patel, K., Bakhurji, A., Salloum, H., Kim, H., Winarno, M., and Mubarak, S. (2018). Use of advanced process control for automating conventional oilfield operations. *Society of Petroleum Engineers - SPE Kingdom of Saudi Arabia Annual Technical Symposium and Exhibition 2018, SATS 2018*, 2020. doi:10.2118/192393-ms.
- Pavlov, A., Krishnamoorthy, D., Fjalestad, K., Aske, E., and Fredriksen, M. (2014). Modelling and model predictive control of oil wells with electric submersible pumps. *2014 IEEE Conference on Control Applications, CCA 2014*, (3905), 586–592.
- Santana, B.A., Fontes, R.M., and Martins, M.A. (2021a). Controlador preditivo de horizonte infinito embar-

- cado: Aplicação hardware-in-the-loop a um sistema de bombeio centrífugo submerso. In *15^o Simpósio Brasileiro de Automação Inteligente*. Rio Grande.
- Santana, B.A., Fontes, R.M., Schnitman, L., and Martins, M.A. (2021b). An adaptive infinite horizon model predictive control strategy applied to an esp-lifted oil well system. *IFAC-PapersOnLine*, 54(3), 176–181. doi: 10.1016/j.ifacol.2021.08.238. 16th IFAC Symposium on Advanced Control of Chemical Processes ADCHEM 2021.
- Zhu, J. and Zhang, H.Q. (2018). A review of experiments and modeling of gas-liquid flow in electrical submersible pumps. *Energies*, 11(1). doi:10.3390/en11010180.